

Increasing Achievable Information Rates via Geometric Shaping

Bin Chen⁽¹⁾, Chigo Okonkwo⁽¹⁾, Hartmut Hafermann⁽²⁾, Alex Alvarado⁽¹⁾

⁽¹⁾ Department of Electrical Engineering, Eindhoven University of Technology, b.c.chen@tue.nl

⁽²⁾ Mathematical and Algorithmic Sciences Lab, Paris Research Center, Huawei Technologies France SASU, 92100 Boulogne-Billancourt, France.

Abstract Achievable information rates are used as a metric to design novel modulation formats via geometric shaping. The proposed geometrically shaped 256-ary constellation achieves SNR gains of up to 1.18 dB.

Introduction

Achievable information rates (AIRs) such as mutual information (MI) and generalized mutual information (GMI) have emerged as practical tools to design fiber optical communication systems. AIRs have also been used to design modulations formats and to predict the performance of forward error correction (FEC)¹.

A key element for maximizing the throughput in both point-to-point links as well as in flexible optical networks is the use of adaptive modulation formats and FEC. Both MI and GMI can be used to analyze this from a theoretical point of view, where GMI is usually preferred due to its practical relevance. The main drawback of the GMI is that the suboptimality of the underlying bit-interleaved coded modulation (BICM) receiver causes a rate loss with respect to the MI. This loss can be eliminated by using BICM with iterative decoding or nonbinary FEC.

Signal shaping can be used in fiber optics to close the gap to the channel capacity, either via probabilistically-shaped (PS) or geometrically-shaped (GS) constellations. In the former, the probabilities of the constellation points are changed²⁻⁶, while in the latter, non-equidistant constellation points are used⁷⁻¹⁰. For the AWGN channel, both schemes achieve Shannon's channel capacity when the number of constellation points tends to infinity. Although PS constellations have superior AIR performance for a finite number of constellation points with respect to GS ones¹¹, this technique requires the use of sophisticated coding. On the other hand, GS rely only on properly placing the constellation points and straightforward modifications of the demapper.

Recently, GS-based constellations such as GS-16QAM⁷, GS-32QAM⁸ and GS-APSK^{9,10} have been investigated in the optical communications literature. GS and PS constellations have also been investigated in the context of the ATSC 3.0

standard¹². GS constellations have even been reported to outperform PS ones in both numerical simulations¹⁰ and experiments⁷. This is particularly noticeable for dispersion managed links^{9,10}. Because of this and the versatility of AIR as design performance metric, in this paper we focus on GS constellations based on both GMI and MI. This paper systematically studies and presents GS constellations with up to $M = 256$ constellation points. We numerically prove that these M -ary constellations with $M = 16, 64, 256$ offer rate gains of up to 7% (or equivalently, SNR gains of up to 1.18 dB) for the AWGN channel.

AIR-based Geometric Shaping Optimization

The largest AIR for a memoryless channel with complex input X and output Y is given by the MI, defined as $I = \mathbb{E}[\log_2 f_{Y|X}(Y|X)/f_Y(Y)]$, where $f_{Y|X}$ is the channel law. An AIR for BICM is the GMI, which is defined as $G = \sum_{i=1}^m \mathbb{E}[\log_2 f_{Y|B_i}(Y|B_i)/f_Y(Y)]$, where B_1, B_2, \dots, B_m represent the bits that are mapped to the channel input X , and $m = \log_2 M$ is number of bits per constellation points.

Both the MI and GMI depend on the channel SNR. The MI depends on the location of the constellation points, and thus, the MI-based optimization problem corresponds to finding the location of M points, that satisfy a power constraint (defining the SNR), and that maximize the MI. The GMI depends also on the binary labeling. The GMI-based optimization problem is thus more complex than the MI one as the binary labeling also needs to be taken into account. In this paper, we use a pairwise optimization algorithm^{8,13} to optimize the MI. For the GMI, we combine it with the binary switching algorithm¹⁴ in an iterative fashion. In both cases the optimization is repeated until the algorithm has converged or a maximum number of iterations is reached.

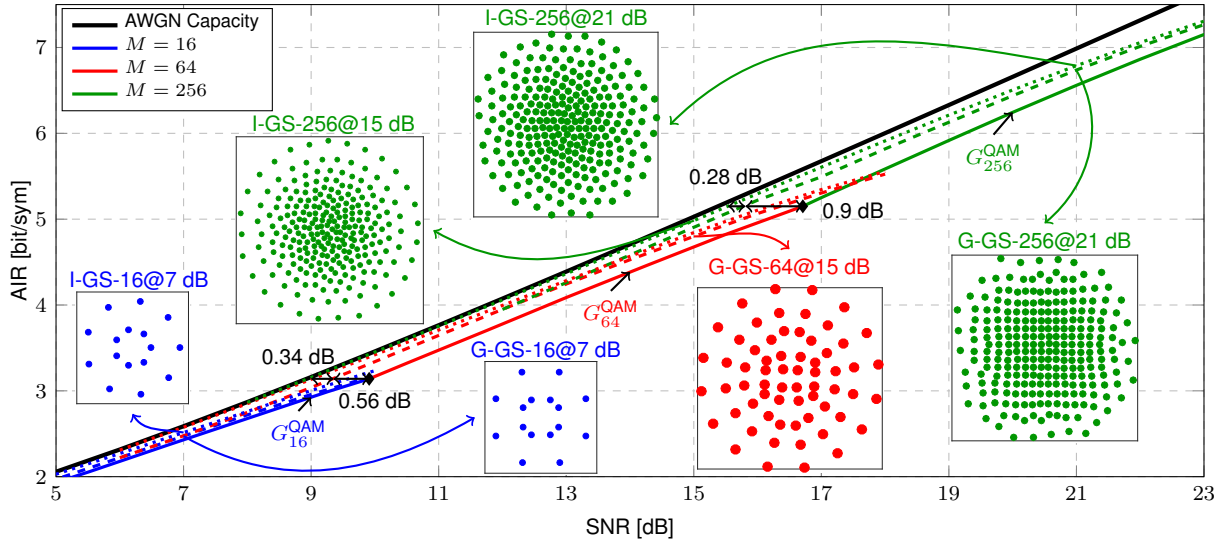


Fig. 1: AIRs of MI-optimized (dotted lines) and GMI-optimized (dashed lines) constellations. The baseline GMIs of MQAM G_M^{QAM} as well as the AWGN capacity (black line) are also shown. Insets: GS-optimized constellations for SNR=7, 15, 21 dB.

Numerical Results: SNR Gains

Here we quantify the SNR gains offered by GS constellations with $M = 16, 64, 256$ over the AWGN channel. As a baseline we use the GMI of square QAM constellations, which are known to cross each other at certain SNR values^{1,10}. This means that depending on the SNR, different modulation formats should be used. This is shown in Fig. 1 (solid lines), where the black diamonds represent the switching points. These three solid lines will be used as baseline, which we denote by G_M^{QAM} . As shown in Fig. 1, we denote each “piece” of this function by G_M^{QAM} .

Dashed lines in Fig. 1 show the GMI of the GMI-optimized constellations for $M = 16$ (blue), $M = 64$ (red), and $M = 256$ (green). Optimized constellations for SNRs 7, 15, and 21 dB are shown as insets (bottom) in Fig. 1, where we use the name G-GS- M to refer to these optimized constellations. At an AIR of 3.14 bit/sym, G-GS-64 gives an SNR sensitivity improvement of 0.56 dB. This gain increases to 0.9 dB at 5.15 bit/sym for G-GS-256. See horizontal black arrows in Fig. 1.

Fig. 2 shows the GMI-optimized constellation G-GS-64@15 dB and its corresponding binary labeling. This constellation achieves 4.8 bits/2D-symbol at 15 dB SNR. The shaded areas in Fig. 2 show the bit-wise decision regions the demapper will use to compute soft bits, where $B_i = 0$ and $B_i = 1$ are shown with white and red resp. This figure shows that the resulting optimized constellation and binary labeling have a highly regular structure.

The MI of MI-optimized GS-modulation formats is also shown in Fig. 1 (dotted lines). Three op-

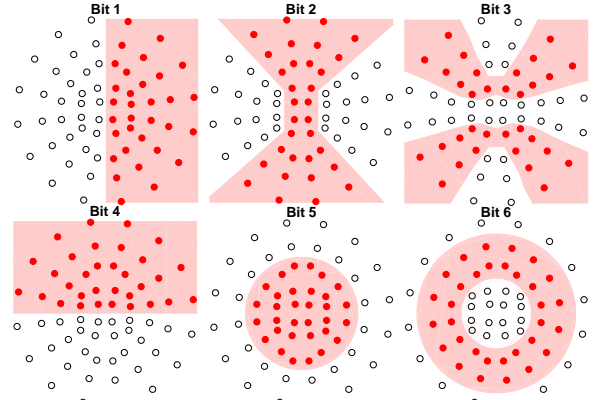


Fig. 2: Constellation and labeling for G-GS-64 for 15 dB. Shaded regions are the decision regions for each bit.

timized constellations (denoted by I-GS- M) are shown in insets in Fig. 1 (optimized for 7, 15 and 21 dB). These results show that AIRs can be further improved by employing MI-optimized GS constellations. For AIRs between 3 and 6 bit/sym, these gains are approximately 0.3 dB over the GMI-optimized GS constellations, and up to 1.18 dB over square QAM. These results highlight the potential gains obtained by using BICM with iterative demapping (or nonbinary FEC) in combination with GS constellations.

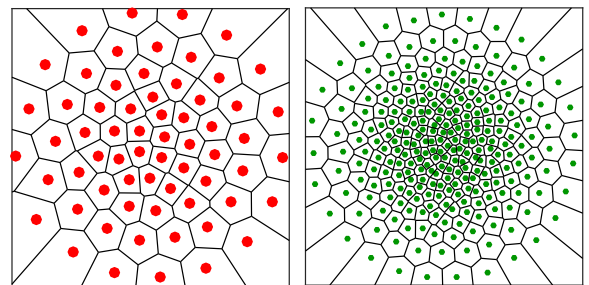


Fig. 3: Constellations I-GS-64 and I-GS-256 for 15 dB.

Fig. 3 shows the MI-optimized constellations

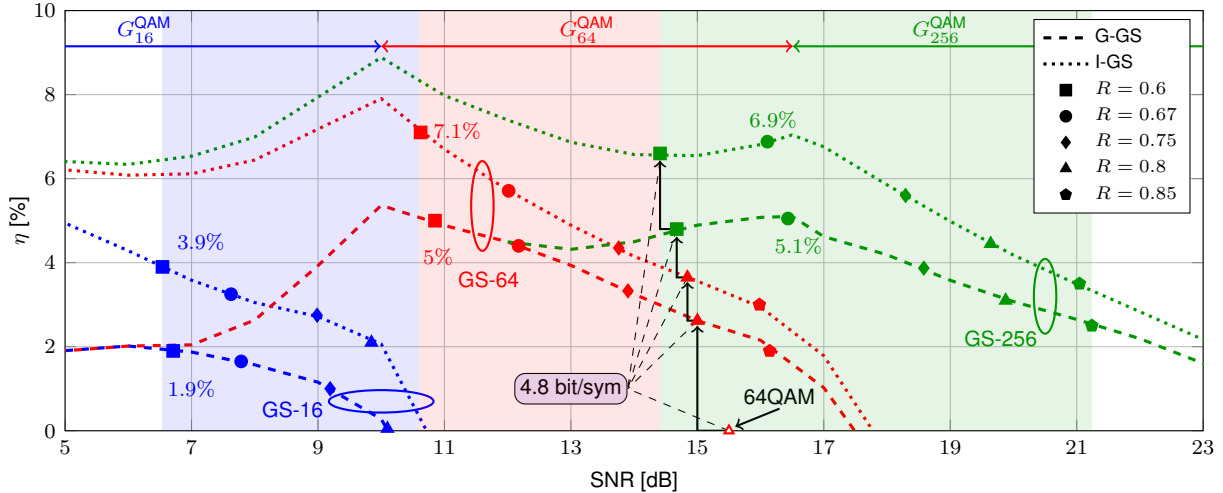


Fig. 4: Relative AIR gains η as a function of SNR. The markers show the relative gain of GS with FEC rates $R = [0.6, 0.67, 0.75, 0.8, 0.85]$. Color-matched shades indicate the optimum SNRs intervals for GS-16, GS-64 and GS-256.

for SNR 15 dB with $M = 64$ and $M = 256$. The Voronoi boundaries indicate the symbol-wise decision regions for the MI-GS formats. For the MI-optimized constellations, these regions are shown to be more circularly symmetric than those of square QAM, which intuitively explains their higher AWGN tolerance. The optimized constellations in Fig. 3 yield MIs of 4.84 bits/2D-symbol and 4.98 bits/2D-symbol, resp. Therefore, the gains with respect to G-GS-64 (dashed red line in Fig. 1) constellations are 0.04 bits/2D-symbol and 0.18 bits/2D-symbol, resp.

Numerical Results: Relative Gains

To better quantify the gains offered by GS constellations, here we consider relative AIR gains with respect to the baseline in Fig. 1 (solid lines). These AIR gains are defined as $\eta = (I^* - G^{\text{QAM}})/G^{\text{QAM}}$ and $\eta = (G^* - G^{\text{QAM}})/G^{\text{QAM}}$, where I^* and G^* represent the AIRs obtained with the optimized constellations.

Fig. 4 shows the obtained relative AIR gains. The dashed curves show the relative gains of GMI-optimized constellations, where the two peaks come from the chosen baseline G^{QAM} (see horizontal arrows in Fig. 4). We also consider the combination of practical FEC rates $0.6 \leq R \leq 0.85$ and GS modulation formats. We observe that GMI-optimized GS constellations with $M = 16, 64, 256$ provide up to 1.9, 5, 5.1% relative AIR gains, resp. This is shown with markers on top of dashed lines in Fig. 4. Interestingly, these maximum gains are obtained for relatively low FEC rates. Fig. 4 also shows the relative gains of MI-optimized GS constellations (dotted lines). The maximum gains in this case are 3.9, 7.1, 6.9% and again obtained for low FEC rates.

The three shaded regions in Fig. 4 show the SNR regions that define which constellation cardinality should be chosen in order to maximize the net data rate if these particular five FEC rates were used. The optimum modulation format switches from GS-16 to GS-64 at a SNR of 10.6 dB and from GS-64 to GS-256 at 14.4 dB.

Lastly, Fig. 4 highlights five combinations of FEC and modulation formats that give the same AIR of 4.8 bit/sym. The first one is square 64QAM (white-filled triangle), which requires 15.5 dB SNR. By using G-GS-64 with $R = 0.8$ (red triangle) and G-GS-256 with $R = 0.6$ (green square), the required SNR is lowered to 15 and 14.84 dB, resp. The last two cases are obtained by considering MI. In this case, the required SNR is further reduced to 14.67 and 14.41 dB for $R = 0.8$ and $R = 0.6$, resp.

Conclusions

We optimized the geometry of constellations based on mutual information and generalized mutual information. The reported constellations result in higher data rates for a wide range of SNRs, different constellation cardinalities, and different FEC overheads. To achieve larger gains, low FEC rates should be considered.

Acknowledgements: This work was supported by Huawei France through the NLCAP project.

References

- [1] A. Alvarado et al., "Achievable Information Rates for Fiber Optics: Applications and Computations," J. Lightw. Technol. 36, 424-439 (2018).
- [2] F. Buchali et al., "Rate Adaptation and Reach Increase by Probabilistically Shaped 64-QAM: an Experimental Demonstration," J. Lightw. Technol. 34, 1599-1609 (2016).
- [3] T. Fehenberger et al., "On Probabilistic Shaping of

- Quadrature Amplitude Modulation for the Nonlinear Fiber Channel," *J. Lightw. Technol.* 34, 5063-5073 (2016).
- [4] G. Bocherer et al., "Fast Probabilistic Shaping Implementation for Long-Haul Fiber-Optic Communication Systems," *Proc. ECOC, Tu.2.D.3* (2017).
- [5] F. Buchali et al., "Spectrally Efficient Probabilistically Shaped Square 64QAM to 256 QAM," *Proc. ECOC, Tu.2.D.1* (2017).
- [6] R. Maher et al., "Constellation Shaped 66 GBd DP-1024QAM Transceiver with 400 km Transmission over Standard SMF," *Proc. ECOC, Th.PDP.B.2* (2017).
- [7] Z. Qu et al., "Geometrically Shaped 16QAM Outperforming Probabilistically Shaped 16QAM," *Proc. ECOC, Th.2.F.4* (2017).
- [8] S. Zhang et al., "Design and Performance Evaluation of a GMI-Optimized 32QAM," *Proc. ECOC, Tu.1.D.4* (2017).
- [9] K. Kojima et al., "Nonlinearity-Tolerant Four-Dimensional 2A8PSK Family for 5-7 Bits/Symbol Spectral Efficiency," *J. Lightw. Technol.* 35, 1383-1391, (2017).
- [10] D. S. Millar et al., "Coded Modulation for Next-Generation Optical Communications," *Proc. OFC, Tu3C.3* (2018).
- [11] L. Szczecinski et al., *Bit-Interleaved Coded Modulation: Fundamentals, Analysis, and Design*, Wiley (2015).
- [12] F. Steiner et al., "Comparison of Geometric and Probabilistic Shaping with Application to ATSC 3.0," *Proc. SCC'17*, (2017).
- [13] B. Moore et al., "Pairwise Optimization of Modulation Constellations for Non-uniform Sources," *IEEE Can. J. Elect. Comput. Eng.*, Vol. 34 (4), (2009).
- [14] F. Schreckenbach et al., "Optimization of Symbol Mappings for Bit-Interleaved Coded Modulation With Iterative Decoding," *IEEE Commun. Lett.*, Vol. 7 (12), p. 593 (2003).